Supplementary Information

The Functional Architecture for Face-processing Expertise: FMRI Evidence of the Developmental Trajectory of the Core and the Extended Face Systems

Frank Haist, Maha Adamo, Jarnet Han, Kang Lee, and Joan Stiles

S1. Introduction

Our study used a novel FMRI data preprocessing technique based on Independent Component Analysis (ICA) to remove structured **P**hysiological noise, **E**ye movement artifact, and **T**ask-**N**egative **A**ctivation, a procedure we refer to as the PETNA method. Removing structured physiological noise (c.f., Perlbarg, et al., 2007) and eye movement artifact (Beauchamp, 2003; Haist, Adamo, Westerfield, Courchesne, & Townsend, 2005; Tregellas, Tanabe, Miller, & Freedman, 2002) via similar methods have been shown previously to significantly improve FMRI task related signal. Using a measure of contrast sensitivity (Thomas, Harshman, & Menon, 2002) with the data presented in this study, we found that structured physiological noise and eye movement artifact removal improved task related signal over the adult, teen, and child groups by 40.12% (SD=15.94%) compared to traditional preprocessing that included motion correction, slice time correction, and spatial smoothing (Haist & Adamo, under review). The truly novel aspect of the technique is the removal of task-negative activity. When task-negative activity was removed, the overall improvement in task-related signal was 113.20% (24.89). Here, we provide a succint overview of the effects of the PETNA technique via a comparison of the average percent signal yielded across all stimulus types for data processed in the traditional manner versus after our PETNA denoising step. Processing for both versions followed the methods detailed in the main text. The only difference is that the "traditional" preprocessing data were taken straight from individual anatomical registration to standardization to the MNI/Talairach brain, while the PETNA "denoised" data underwent the additional steps to identify and remove physiological noise, eye artifact, and task-negative activation as detailed in the main methods text. The aim of the comparison between the traditional and PETNA denoised versions is to demonstrate the whole-brain effects of our extended processing, namely increases in measures of task-related activity overall.

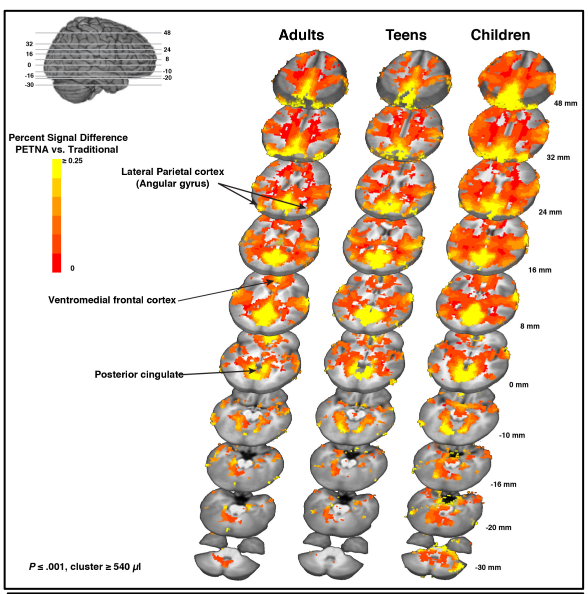

Fig. S1 Regions where PETNA processed data produced reliably greater task-related activation compared to Traditional preprocessing for adults, teens, and children separately. Regions typically associated with the "Default Mode Network" (DMN) are highlighted. Note that improved signal extended beyond the DMN regions indicating that PETNA identifies other task negative activity in addition to DMN.

S2. Methods

Data from all participants reported in the main text were included in these analyses. Section 2.5.1 of the main paper describes the PETNA method. The traditional preprocessing version had no additional steps between anatomical registration and template standardization. Both versions underwent the analyses characterized in Section 2.5.3, namely deconvolution and regression of the BOLD data and subsequent conversion of regression weights into percent signal scores for each of the four stimulus types presented in the task. We calculated the mean of the percent signal scores across stimulus types per processing version per participant, yielding two functional intensity maps per participant (traditional and PETNA preprocessed). These maps were submitted to separate repeated measures ANOVAs for each age group with preprocessing version (fixed effect) and participant (random effect nested within preprocessing version) as factors. We then calculated BOLD activity (percent signal) that was greater in the PETNA preprocessing than in the traditional preprocessing data. The results were thresholded at $P \leq .001$ with a minimum activation cluster of 540 µl (20 contiguous voxels). These results are shown in **Figure S1**. The group results were binarized and group masks for children and adults were overlaid to create conjunction maps of activity that showed regions where the PETNA process produced significant activity in children only, adults only, and where increased activity was observed for both children and adults. These maps are shown in **Figure S2**.

S3. Results

As shown in **Figure S1**, all three age groups exhibited greater task-related signal in the PETNA processed data relative to Traditional preprocessing. Regions commonly associated with the default mode network (DMN) are highlighted in Fig. S1. The PETNA process improved task-related signal in all of these regions. However, the extent of signal improvement included substantially more regions than those in the DMN. This suggests that the PETNA process identifies additional sources of task-negative activation and provides improved task-related signal widely distributed across cortical and subcortical regions. These results further suggest that the benefit in task-related signal has a broader spatial distribution in children compared to adults.

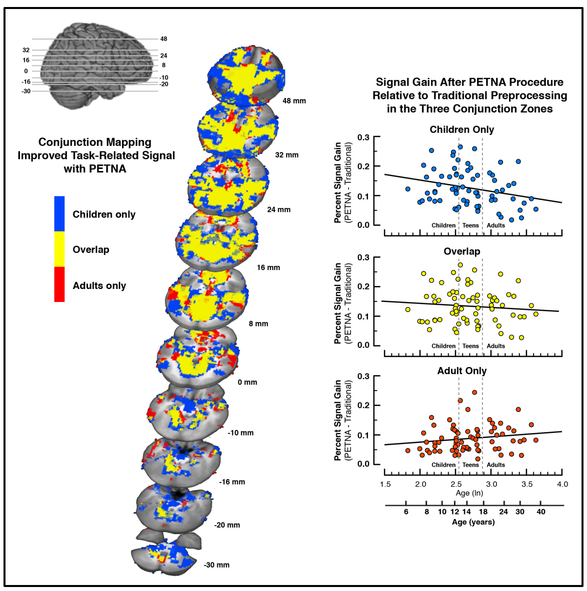

Fig S2 Left Panel: conjunction map showing regions with significantly improved task-related signal for adults or children only, or regions with improved signal for both groups. Children showed a greater benefit for improved signal across the brain. **Right Panel**: Improved signal within conjunction regions as a continuous measure of age (including teens). There was a significant positive effect for age only in the voxels showing “child only” improved task-related signal. In the other regions, all participants benefited equivalently.

Figure S2-left panel presents the results from Fig. S1 in a different format, as a conjunction map showing regions in which both adults and children produced greater task-related signal in the PETNA data, regions where only children showed improved signal, and regions where only adults showed improved signal. There was a significant degree of overlap in the improved signal for adults and children with a total of 412,965 µl of shared activity gain (yellow regions). However, children showed much greater benefit from the PETNA procedure with an additional 316,953 µl of brain activation showing significantly improved signal (blue regions). Adults showed a modest 79,974 µl of unique brain activation improvement (red regions). In other words, the PETNA procedure improved task-related signal in children in nearly double the brain that showed common effects with adults.

Figure 2-right panel shows the signal improvement in each of the conjunction map regions as a

continuous measure of age (natural logarithm transformed). These data include the teen participants. Separate regressions against the natural logarithm of age tested the difference in percent signal improvement following the PETNA procedure in each of the conjunction map areas. Significant decreases with age were seen only for child-only voxels (R^2 = .068, $F_{1, 69}$ = 5.06, P = .03) and no effect of age was observed for adult-only voxels (R^2 = .027, $F_{1, 69}$ = 1.90, P = .17) or overlapping voxels (R^2 = .009, $F_{1, 69}$ = 0.66, P = .42).

S4. Discussion and Conclusion

The removal of physiological noise, eye artifact, and task-negative activity with our PETNA procedure produced significant increases in task-related signal for all age groups tested, with benefits of this denoising procedure notably centered around and extending beyond areas of the default mode network. Furthermore, the gains in task-related percent signal were greater for children than for adults, particularly with respect to the spatial extent of areas showing increased signal following denoising. A more complete discussion of the implications of this denoising technique is available elsewhere (Haist & Adamo, under review), but the most relevant point here is that different age groups show different levels of default mode activity that contribute to the "baseline" periods of the task (Fair, et al., 2008; Fair, et al., 2009; Supekar, et al., 2010) and potentially skew the observed task results. In these supplemental analyses, we see the potential effects of those differences; the correction of this likely confound promotes a more accurate assessment of age-related effects, as reported in the main text, and should prove useful for comparisons of data from any populations that could potentially differ with respect to structured noise.

References Cited

Beauchamp, M. S. (2003). Detection of eye movements from fMRI data. *Magnetic Resonance in Medicine, 49*, 376-380.

Fair, D. A., Cohen, A. L., Dosenbach, N. U., Church, J. A., Miezin, F. M., Barch, D. M., Raichle, M. E., Petersen, S. E., & Schlaggar, B. L. (2008). The maturing architecture of the brain's default network. *Proceedings of the National Academy of Sciences of the United States of America, 105*, 4028-4032.

Fair, D. A., Cohen, A. L., Power, J. D., Dosenbach, N. U., Church, J. A., Miezin, F. M., Schlaggar, B. L., & Petersen, S. E. (2009). Functional brain networks develop from a "local to distributed" organization. *PLoS Computational Biology, 5*, e1000381.

Haist, F., & Adamo, M. (under review). A preprocessing procedure to remove Physiological noise, Eye movement artifact, and Task-Negative Activity from FMRI data: The PETNA procedure.

Haist, F., Adamo, M., Westerfield, M., Courchesne, E., & Townsend, J. (2005). The functional neuroanatomy of spatial attention in autism spectrum disorder. *Developmental Neuropsychology, 27*, 425-458.

Perlbarg, V., Bellec, P., Anton, J. L., Pelegrini-Issac, M., Doyon, J., & Benali, H. (2007). CORSICA: correction of structured noise in fMRI by automatic identification of ICA components. *Magnetic Resonance Imaging, 25*, 35-46.

Supekar, K., Uddin, L. Q., Prater, K., Amin, H., Greicius, M. D., & Menon, V. (2010). Development of functional and structural connectivity within the default mode network in young children. *Neuroimage, 52*, 290-301.

Thomas, C. G., Harshman, R. A., & Menon, R. S. (2002). Noise reduction in BOLD-based fMRI using component analysis. *Neuroimage, 17*, 1521-1537.

Tregellas, J. R., Tanabe, J. L., Miller, D. E., & Freedman, R. (2002). Monitoring eye movements during fMRI tasks with echo planar images. *Human Brain Mapping, 17*, 237-243.